Martian Dust Storm Spatial-Temporal Analysis of Tentative Landing Areas for China's Tianwen-3 Mars Mission. Yuan Tian[1], Bo Li[1*], Zhaojin Rong[2], Shaojie Qu[3], Shengbo Chen[4], [1]Shandong Provincial Key Laboratory of Optical Astronomy and Solar-Terrestrial Environment, Institute of Space Sciences, Shandong University, Weihai, China, [2]Key Laboratory of Earth and Planetary Physics, Institute of Geology and Geophysics, Chinese Academy of Sciences, Beijing, China, [3]Beijing Institute of Spacecraft System Engineering, Beijing, China, [4]College of Geoexploration Science and Technology, Jilin University, Changchun, China.

Introduction: Tianwen-3, China's first Mars sample return Mission, is scheduled to launch and retrieve samples around 2030. Three tentative landing areas, referred to as TLAs (Amazonis, Chryse and Utopia Planitiae, i.e., TLA-A, TLA-C and TLA-U), have been selected based on elevation <−2,000 m and latitude between 17° and 30°N (Fig.1). Despite the extreme thinness of the Martian atmosphere and its low atmospheric pressure, there is no lack of active atmospheric phenomena. Due to the characteristics of Mars' orbit (high eccentricity), the Martian atmosphere exhibits explicit seasonal variations. As the most dramatic atmospheric activities, dust storms occur in all seasons on Mars and affect the accuracy and safety of Mars exploration missions. As early as the 18th and 19th centuries, previous researchers observed phenomena such as the changes in polar ice caps, "white and blue" clouds, and "yellow clouds or hazes" [1-4] through Earth-based observations, and "the yellow clouds" were associated with Martian dust storms [4]. After that, Earth-based telescopes, orbiters in Mars orbit, and landers and rovers provided more details about dust storms. The Mars Global Surveyor's (MGS) Mars Orbiter Camera (MOC) carried the wide-angle imager to observe surface changes like albedo and polar caps and atmospheric phenomena such as dust storms and condensate clouds.

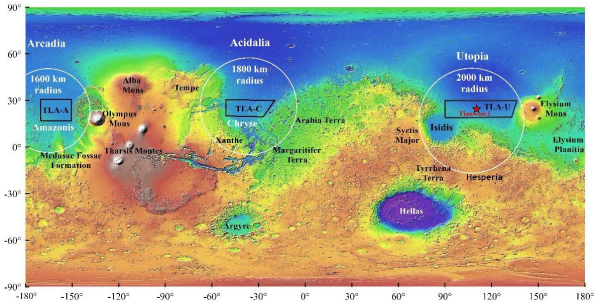

Fig.1. Three tentative landing areas (TLAs) for the Tianwen-3 mission. The base map is the Mars Orbiter Laser Altimeter (MOLA) colorhillshade map in simple cylindrical projection. The black polygons indicate the locations of the three TLAs, while the white circles represent their monitoring rings.

In this paper, we utilized Mars Daily Global Maps (MDGMs) captured by the MOC to detect dust storms around three TLAs in five consecutive Mars years (MY 24-28). We focused on mapping the spatial-temporal distributions of dust storm activities during the Tianwen-3 mission to designate safe landing areas and determine the preferred entry-descent-landing (EDL) as well as take-off and ascent (TOA) periods for the Tianwen-3 mission.

Data and Methods: Each of the wide-angle (WA) cameras of the MOC provides a 140° field of vision with red (575-625 nm) and blue (400-450 nm) band passes (WAR and WAB) to produce global map swaths [5]. Data used in this work are the MOC MDGMs produced from daily mosaics of MOC global map swaths in a simple cylindrical projection, between June 1999 (MY 24) and October 2006 (MY 28).

To effectively analyze the spatial-temporal correlation between dust storms and their impact on landing areas, we utilized a visual inspection method to identify dust storms around the three TLAs. First, we monitored the daily surface albedo in the study area and extracted regions with albedo variations. Second, the changing morphology and colors in the images were used to distinguish between dust storms and diffuse clouds. Finally, condensation clouds (ice) and dust storms were characterized based on the difference in brightness of the images in the blue and red bands. After identifying the dust storms, we used the simple cylindrical projection to measure shape parameters.

Results: We observed 2476 dust storms across the three TLAs, with 565 dust storms occurring in TLA-A, TLA-C, and TLA-U (115, 245, and 205, respectively).

Temporal probabilities of dust storm activity within three TLAs. Drawing on the previous studies [6,7], we defined the proportion of the average daily occurrence of dust storms over multiple Mars years to the study area as the temporal probability of dust storm occurrence on that Ls, as shown in Fig.2, symbolized as $P(T)$. According to the two potential launch scenarios for the Tianwen-3 mission, two pre-selected mission periods, the T_1 period (Ls=161–309°) and T_2 period (Ls=342–55°) are chosen for dust storms spatial-temporal analysis in this paper [8]. Dust storms within three TLAs exhibited noticeable seasonality and inhomogeneity throughout a Mars year, manifesting pronounced periods of solstitial pauses, and the distribution pattern of $P(T)$ showed a strong correlation with the advance and retreat of the seasonal ice cap.

The average $P(T)$ within TLA-A, TLA-C and TLA-U during the T_1 period were 1.90%, 5.61% and 2.69%, respectively. During the T_2 period, these values were 0.22%, 1.01% and 0.58%, respectively. Consequently, we think the T_2 period is more suitable for the Tianwen-3 mission than the T_1 period.

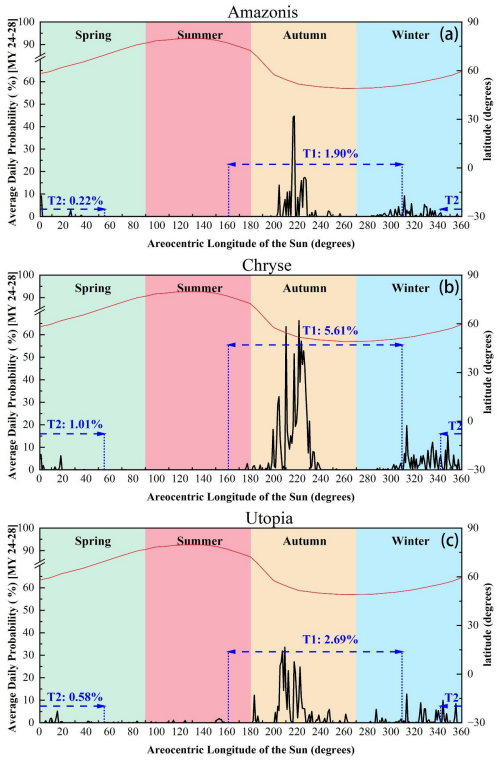

Fig.2. Average daily probability versus Ls distributions of dust storm activity within three TLAs in MY 24-28 binned in 1° of Ls. (a), (b) and (c) denote the TLA-A, TLA-C and TLA-U, respectively. The horizontal axis indicates the Ls, the left vertical axis represents the dust storm probability (black curve), and the right vertical axis is the average latitude at the edge of the northern polar ice cap (red curve).

Spatial Probabilities of Dust Storm Activity Within Three TLAs during T_2. We divided the three monitoring rings (around the three tentative landing areas) into regular square grids with 0.5° latitude × 0.5° longitude and counted the average spatial probability of dust storm occurrence, denoted as $P(S)$. Fig.3. showed $P(S)$ distribution characteristics within TLAs: higher probabilities in the northern and central areas and lower probabilities in the southern and peripheral regions. The spatial distribution of dust storms within the three study areas may result from a combination of topography (negatively correlated), dust storm origins, the route of dust storm sequences, and the expansion and contraction of seasonal ice caps.

Preferred EDL & TOA Periods and Safe Landing Areas. We split T_2 into two phases: EDL phase (Ls=342-18°) and TOA phase (Ls=19-55°), and then select Ls=2-18°, Ls=4-12°, and Ls=356-4° as the suggested EDL times for TLA-A, TLA-C, and TLA-U, respectively, and Ls=45-55° as the suggested TOA time. According to previous research on the first Mars exploration mission of China [7,9-12] and the international Mars exploration mission [13-15], and combining engineering constraints and scientific factors, we selected five safe landing areas (Fig.3, radius=50 km) where the probability of dust storms is <3%, The average $P(S)$ of A1, C1, C2, U1 and U2 are 0%, 1.33%, 0.67%,1.49% and 0.62%.

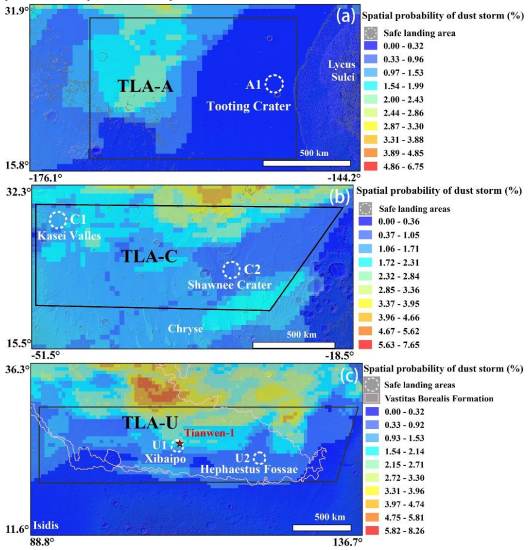

Fig.3. Spatial distributions of dust storms within three TLAs during the T_2 period, split into grids of 0.5°, overlaid the MOLA colorhillshade map. (a), (b) and (c) denote the Amazonis, Chryse and Utopia study areas, respectively. Five safe landing areas have been selected, labeled A1, C1, C2, U1 and U2.

References: [1] Capen, C. F., & Martin, L. J. (1971). THE DEVELOPING STAGES OF THE MARTIAN YELLOW STORM OF 1971. [2] Flammarion, C. (1892). Gauthier-almmarion. Willars et fils. [3] McKim, R. J. (1999). Journal of the British Astronomical Association, 109(5), 286–287. [4] Prey, A. (1931). Monatshefte Für Mathematik Und Physik, 38–38(1), A17–A17. [5] Malin et al., (1992). JGR, 97(E5), 7699–7718. [6] Cantor et al., (2019). Icarus, 321, 161-170. [7] Yao et al., (2020). Earth and Space Science, 7(8). [8] Jones, A. (2022). SpaceNews. [9] Li et al., (2021). Universe, 7(11), 433. [10] Luo et al., (2021). RS, 13(11), 2206. [11] Qu et al., (2021). RS, 14(1), 8. [12] Y. Wang et al., (2021). RS, 13(13), 2601.[13] Golombek et al., (2012). Space Science Reviews, 170(1–4), 641–737. [14] Golombek et al., (2012). In Space Science Reviews (Vol. 211, Issues 1–4, pp. 5–95). [15] Vago et al., (2015). Solar System Research, 49(7), 538–542.